



Targeted Molecular Screening of Fungal Metabolites for Blocking *Rabies lyssavirus* Infection Mechanisms

Charles Justine P. Meroy, Reina Jessica C. Lim, Kristina Casandra C. Liwag, Jean Rodrique F. Maranca, Denise Joyce H. Maximo, Kirby O. Morales, Jenny Rose B. Nalidong, Mary Rose F. Lirio*

Department of Medical Technology, Institute of Health Sciences and Nursing, Far Eastern University, Nicanor Reyes Street, Sampaloc, 1008 Metro Manila, Philippines

*Corresponding Author's Email: mlirio@feu.edu.ph / maryroselirio@gmail.com

Abstract

Rabies is a fatal viral disease transmitted to humans primarily through the saliva of infected animals via bites or scratches. With limited treatment options currently available, *Rabies lyssavirus* (RABV) continues to pose a serious public health concern. This study explored the potential of fungal metabolites as antiviral agents against RABV by evaluating their in-silico interactions with four key viral proteins: glycoprotein (RABV-G), RNA-dependent RNA polymerase (RABV-L), phosphoprotein (RABV-P), and matrix protein (RABV-M). A total of fifty-two (52) fungal metabolites were screened using molecular docking, of which eighteen (18) compounds demonstrating high binding affinities were further assessed for physicochemical and pharmacokinetic properties. Notably, Chaetoglobosin A and Cladosporone B showed strong interactions with both RABV-G and RABV-L, while Chaetoglobosin C achieved the most favourable binding affinities overall. ADMET profiling indicated that most of the selected metabolites exhibited favourable pharmacokinetic characteristics; however, limited blood-brain barrier (BBB) permeability and variable bioavailability highlight the need for structural optimisation. These findings suggest that fungal metabolites—particularly Chaetoglobosin C—hold significant promise as antiviral candidates against RABV. Further in vitro and in vivo validation will be required to confirm their clinical and therapeutic potential.

Keywords: Antiviral Drugs; Chaetoglobosin C; Fungal Metabolites; *Rabies lyssavirus*

Introduction

Rabies remains a major global health concern, particularly in regions of Africa and Asia, where domestic dog bites account for the majority of human cases (Ling *et al.*, 2023). Transmission usually occurs through the saliva of infected animals such as dogs, cats, monkeys, and bats via bites or scratches (Fisher *et al.*, 2018). According to the World Health Organization (2024), rabies is responsible for tens of thousands of preventable deaths each year, highlighting the urgent need for novel therapeutic interventions. Current post-exposure prophylaxis (PEP) is effective only when administered promptly, and its use is limited in resource-constrained settings where access to vaccines may be restricted (Quiambao *et al.*, 2020). Furthermore, once clinical symptoms develop, PEP is no longer effective (Kimitsuki *et al.*, 2022).

Rabies lyssavirus (RABV), the aetiological agent of rabies, enters through the peripheral nervous system (PNS) and spreads to the central nervous system (CNS), where it causes fatal encephalitis and progressive neurological symptoms (Fatima *et al.*, 2023). Without timely intervention, the infection results in irreversible CNS damage, ultimately leading to paralysis, coma, and death (Kimitsuki *et al.*, 2022).

The viral life cycle relies on several essential proteins. The surface glycoprotein (RABV-G) mediates host cell receptor recognition and membrane fusion, whilst also modulating immune responses (Lian *et al.*, 2022). The phosphoprotein (RABV-P) acts as a chaperone for RNA-free N (N0) protein, preventing inappropriate RNA binding, whilst simultaneously antagonising host interferon signalling (Zhan *et al.*, 2024). The matrix protein (RABV-M) plays a pivotal role in virion assembly and enhances replication efficiency by suppressing transcription (Yuan *et al.*, 2024). Finally, the RNA-dependent RNA polymerase (RABV-L) catalyses viral RNA synthesis and replication (Rampersad & Tennant, 2018). Collectively, these proteins represent attractive molecular targets for antiviral development, as their inhibition could disrupt viral replication and disease progression. Fungal secondary metabolites, recognised for their broad bioactive potential, have been reported to exhibit antiviral activity by interfering with viral entry and replication pathways (Louten, 2016). However, their potential against RABV remains largely unexplored. This study therefore investigates the inhibitory potential of fungal metabolites against RABV proteins through molecular docking approaches. By screening fifty-two (52) fungal metabolites and evaluating their interactions with key viral proteins, this study aims to identify promising candidates for the development of antiviral treatments against rabies.

Materials and Methods

Selection of Target Proteins and Ligands

The viral proteins selected for this study are summarised in Table 1, which outlines their specific biological functions and provides justification for their inclusion as key targets in molecular docking analyses. The three-dimensional (3D) structures of four Rabies lyssavirus (RABV) proteins were retrieved in PDB format from the Protein Data Bank (<https://www.rcsb.org>). These proteins were prioritised due to their essential roles in viral entry, replication, immune evasion, and host–virus interactions, making them critical candidates for antiviral intervention.

Accordingly, fifty-two (52) fungal secondary metabolites were selected based on reported bioactive properties and documented antiviral potential. Their three-dimensional (3D) structures were obtained in SDF format from PubChem (<https://pubchem.ncbi.nlm.nih.gov>). These compounds were chosen to evaluate their potential as RABV inhibitors, particularly in light of the growing recognition of fungal metabolites as promising candidates for drug discovery.

Table 1: List of the Target Proteins Used in the Study

Protein	Function/s	PDB ID
RABV-G (Glycoprotein)	Mediates viral attachment and entry into host cells via receptor binding and membrane fusion	8A1E
RABV-M (Matrix Protein)	Regulates viral assembly and budding; plays a role in host immune evasion	1VYI
RABV-L (RNA-dependent RNA Polymerase)	Catalyzes viral RNA replication and transcription	6UEB
RABV-P (Phosphoprotein)	Functions as a cofactor for the L protein, facilitating RNA synthesis and host immune suppression	7C20

Preparation of Target Proteins and Ligands

The preparation of the selected fungal metabolites (ligands) and Rabies lyssavirus proteins was performed using UCSF Chimera. As described by Pettersen *et al.* (2004), this software enables the optimisation of molecular structures, refinement of ligand and receptor conformations, removal of water molecules, and assignment of charges prior to docking simulations.

The three-dimensional (3D) crystal structures of the target Rabies lyssavirus proteins (Table 1) were retrieved from the Protein Data Bank (PDB) and subsequently prepared using UCSF Chimera. Non-standard residues, including water molecules and metal ions, were removed to prevent interference with ligand binding. Hydrogen atoms were then added, and Gasteiger charges were assigned through Amber's Antechamber module to stabilise molecular structures. To ensure docking accuracy, HOH

groups were excluded, and specific hydrogen atoms were reintroduced at critical sites to preserve essential secondary and tertiary structures (Zhang *et al.*, 2021).

Ligand preparation involved optimising 3D conformations, adding hydrogen atoms for structural stability, and refining electrostatic properties. Impurities were removed, and Gasteiger charges were applied to enhance electrostatic interactions with receptor proteins. Both protein and ligand structures were converted into the PDBQT format using AutoDock Tools, as required for docking in AutoDock Vina.

Molecular Docking of Protein-Ligand Interactions

Molecular docking simulations were carried out using AutoDock Vina to evaluate the binding interactions between the prepared fungal metabolites and Rabies lyssavirus proteins. This approach estimates binding affinities and predicts the most favourable ligand orientations within macromolecular targets.

The docking procedure involved defining the active site of each protein and configuring a grid box around the predicted binding pocket to generate multiple ligand–protein binding poses. The Broyden–Fletcher–Goldfarb–Shanno (BFGS) algorithm was applied to iteratively refine ligand conformations by minimising system free energy. By adjusting ligand atom positions and torsional angles within the binding site, the algorithm identifies stable conformations at local energy minima.

Docking results were evaluated by assessing binding energies and root-mean-square deviation (RMSD) values. RMSD thresholds of ≤ 2 Å were considered acceptable, as conformations within this range are regarded as highly reproducible. Binding affinities were interpreted on the basis of docking scores, with values below -6 kcal/mol indicating effective binding, and scores between -8 and -12 kcal/mol suggesting particularly strong interactions.

Post-docking Analyses of Protein-Ligand Interactions

Post-docking analyses were performed to further evaluate the stability and binding effectiveness of the predicted protein–ligand complexes. BIOVIA Discovery Studio was used to characterise critical interactions, including hydrogen bonding, hydrophobic interactions, van der Waals forces, and electrostatic contacts.

Hydrogen bonds were assessed based on donor–acceptor distances and bond angles, with values below 3.5 Å and angles approaching 120° – 180° considered optimal. Hydrophobic interactions were examined to determine the sequestration of non-polar moieties into hydrophobic pockets, whilst van der Waals forces were evaluated for short-range stabilisation. Electrostatic interactions were also analysed to confirm Coulombic attractions between charged groups on the ligands and target proteins.

The most stable ligand–protein complexes were identified by comparing their binding energy scores and RMSD values. Complexes with the lowest binding energies and RMSD values ≤ 2 Å were considered to represent the most stable and reproducible binding conformations.

Absorption, Distribution, Metabolism, and Excretion Properties of Fungal Metabolites

Following docking analysis, selected fungal metabolites were subjected to pharmacokinetic profiling using SwissADME to predict Absorption, Distribution, Metabolism and Excretion (ADME) properties. Since pharmacokinetic behavior strongly influences therapeutic potential, this step was essential to evaluate whether the compounds could be efficiently absorbed, distributed, metabolized, and excreted.

A key part of this analysis was Lipinski's Rule of Five, which provides guidelines for predicting drug-likeness and oral bioavailability. According to Lipinski *et al.* (2001), compounds with more than five hydrogen bond donors, more than ten hydrogen bond acceptors, a molecular weight greater than 500 Daltons (Da), or a Log P (cLogP) value exceeding five are likely to exhibit poor oral bioavailability. Compounds exceeding these thresholds were flagged for potential limitations in solubility, membrane permeability, or absorption.

BOILED-Egg Model

The BOILED-Egg predictive model was applied to assess gastrointestinal (GI) absorption and blood–brain barrier (BBB) penetration. This model integrates lipophilicity (WLOGP) and total polar surface area (TPSA) to classify compounds visually. Molecules located in the “white” region of the model are predicted to have good GI absorption, whereas those positioned in the “yolk” region are considered capable of crossing the BBB. These properties provide valuable insight into the oral suitability of compounds as well as their potential to act on central nervous system (CNS) targets.

Physicochemical and Toxicological Evaluation

The physicochemical properties and toxicity risks of the selected metabolites were evaluated using OSIRIS Property Explorer. Several key parameters were analysed to determine their drug-likeness. An ideal total polar surface area (TPSA) was considered to be $\leq 140 \text{ \AA}^2$, while cLogP values in the range of -0.4 to 5.6 indicated a favourable balance of solubility and lipophilicity. Solubility ($\log S$) was also assessed, with values between -1 and -5 regarded as optimal for absorption in biological systems. In addition, molecular weight values between 160 and 500 Da were considered suitable for oral drug development.

Each compound was further screened for potential mutagenicity, tumorigenicity, irritancy, and reproductive toxicity. Molecules predicted to present significant toxicological risks were deprioritised for further evaluation.

Results

Binding Affinity of the Target Proteins and Fungal Metabolites

A total of eighteen (18) fungal metabolites demonstrated high binding affinity towards the major structural proteins of Rabies lyssavirus (RABV), all of which are directly involved in viral entry and replication. The binding affinity scores for these protein–ligand interactions are summarised in Table 2, providing an overview of the docking outcomes across the four (4) viral protein targets.

From this screening, three (3) compounds emerged as the most promising candidates, exhibiting the strongest binding affinities across multiple targets. These lead compounds were subsequently selected for post-docking analysis, as detailed in Table 3. This approach facilitated the prioritisation of fungal metabolites with the greatest therapeutic potential for further structural investigation.

Table 2: Binding Energies (kcal/mol) of Fungal Metabolites (1–18) Against Target Proteins of Rabies lyssavirus

Fungal Metabolites	Biological Activity	RABV-G	RABV-L	RABV-P	RABV-M
Aspergilline A (1)	Antibacterial properties and antifungal activity	-8.8	-9.7	-7.9	-6.7
Ergosterol peroxide (2)	Antibacterial and antiviral activity	-8.6	-9.6	-6.9	-6.7
Sterigmatocystin (3)	Cytotoxicity and antifungal activity	-8.7	-8.5	-6.4	-6.1
Brevianamide A (4)	Antifungal and antibacterial activities	-8.8	-9.4	-7.7	-7.7
Cochliodinol (5)	Antifungal activity and cytotoxic effects	-9.4	-9.8	-7.8	-7.6
Viriditoxin (6)	Antiviral and antifungal properties	-8.1	-8.0	-6.6	-7.1
Palmarumycin C11 (7)	Antibacterial and antiviral properties	-7.9	-9.7	-7.5	-7.7
Palmarumycin C12 (8)	Antiviral and antifungal properties	-9.0	-10.1	-6.9	-7.2
Cladospirone B (9)	Antibacterial and antifungal properties	-9.9	-10.1	-7.2	-7.2
Chaetoglobosin A (10)	Cytotoxic and antiviral activities	-9.8	-10.2	-7.8	-8.0

Chaetoglobosin C (11)	Cytotoxic and antiviral effects	-10.1	-12.4	-7.9	-7.8
Chaetomugilin A (12)	Cytotoxic and antiviral properties	-8.0	-9.2	-6.7	-7.4
Chaetomugilin B (13)	Antiviral and cytotoxic activities	-7.9	-9.2	-6.6	-7.0
Chaetoglobosin D (14)	Antiviral and cytotoxic effects	-9.3	-10.0	-7.9	-7.3
Helvolic acid (15)	Antibacterial and antifungal activities	-6.9	-7.8	-5.9	-6.2
Chetomin (16)	Antiviral and antifungal properties	-8.2	-11.1	-7.0	-7.5
Stachybotrin C (17)	Antifungal and antiviral properties	-9.7	-8.6	-7.3	-8.0
Tryptoquivaline (18)	Antiviral and cytotoxic activities	-7.8	-9.2	-7.0	-6.7

Table 3: Top Three (3) Compounds with the Strongest Binding Affinity to Four (4) Target Proteins

Target Protein	Compound	Binding Affinity (kcal/mol)
RABV-G	11	-10.1
	9	-9.9
	10	-9.8
RABV-L	11	-12.4
	16	-11.1
	12	-10.2
RABV-P	1	-7.9
	11	-7.9
	14	-7.9
RABV-M	10	-8.0
	17	-8.0
	11	-7.8

Post-docking Analysis with RABV-G

The *Rabies lyssavirus* glycoprotein (RABV-G) is a critical determinant of viral entry, mediating attachment and membrane fusion, and therefore represents an important antiviral target. Molecular docking analysis identified several fungal metabolites with strong affinities for RABV-G (Table 4). Among these, Chaetoglobosin C (-10.1 kcal/mol), Cladospirone B (-9.9 kcal/mol), and Chaetomugilin A (-9.8 kcal/mol) displayed the most favourable binding energies, indicating a strong potential to inhibit glycoprotein function and block viral entry.

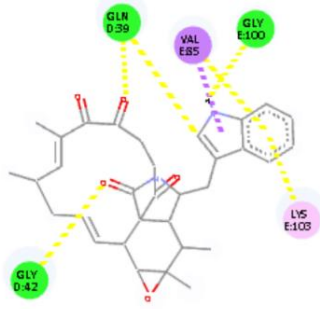
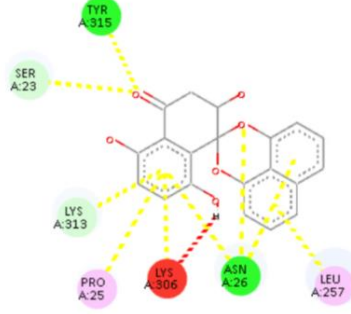
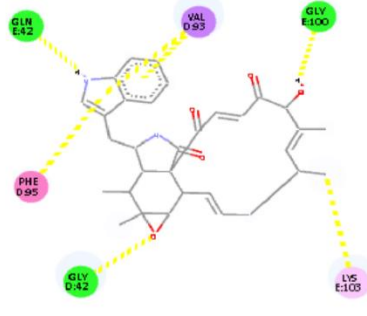
Chaetoglobosin C (11), a metabolite of *Chaetomium globosum* with established antiviral properties (Song, 2024), demonstrated strong binding through hydrogen bonds with GLN39, GLY42, and GLY100. Its stability was further reinforced by π -sigma and π -alkyl hydrophobic interactions with VAL85 and LYS103. Similar interaction patterns have previously been reported in fungal alkaloids targeting the SARS-CoV-2 spike glycoprotein (Alanzi *et al.*, 2023); likewise, Qaisrani *et al.* (2021) showed that a combination of hydrophobic contacts and hydrogen bonds stabilised ligand-glycoprotein complexes, underscoring Chaetoglobosin C's potential as an RABV-G inhibitor.

Cladospirone B (9), derived from *Cladosporium* species, exhibited a binding affinity of -9.9 kcal/mol. Its interactions included π -donor hydrogen bonds with LYS313 and ASN26, complemented by hydrophobic contacts with PRO25, LYS306, and LEU257. By potentially hindering the conformational shifts required for glycoprotein-mediated fusion, these interactions resemble inhibitory mechanisms previously reported for Dengue virus glycoprotein inhibitors (Lee *et al.*, 2023). Moreover, as Salvatore

et al. (2021) highlighted, *Cladosporium*-derived metabolites constitute a valuable source of antiviral agents, reinforcing the relevance of Cladospirone B in anti-rabies strategies.

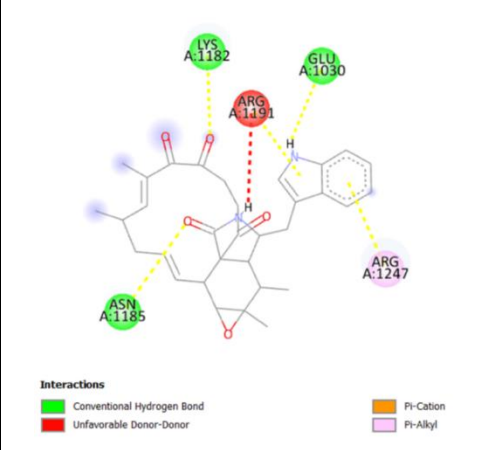
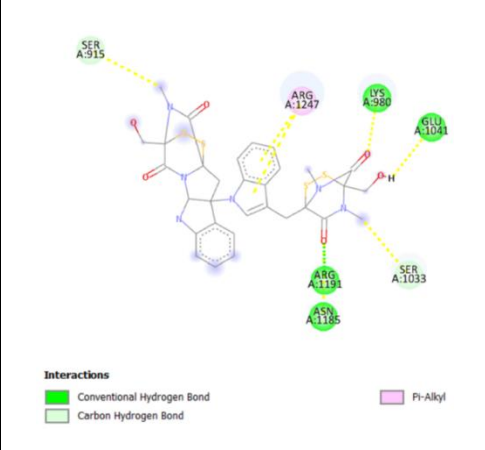
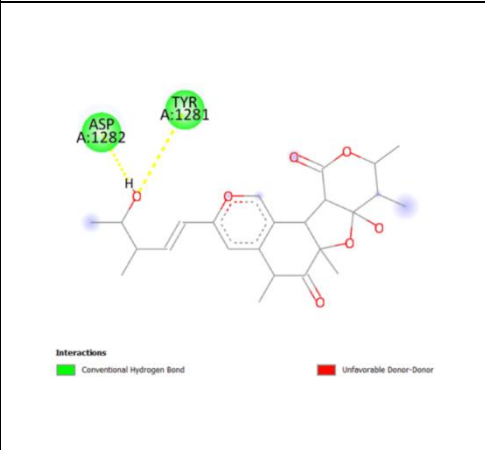
Chaetoglobosin A (**10**) also demonstrated strong binding to RABV-G (−9.8 kcal/mol), forming hydrogen bonds with GLY42, GLN42, and GLY100, together with hydrophobic interactions involving VAL93, PHE95, and LYS103. The resulting stable complex reflects a binding mode commonly observed in viral entry inhibitors, including those targeting HIV gp41 and the SARS-CoV-2 spike protein, where aromatic-rich scaffolds stabilise interactions within fusion-relevant sites (Desantis *et al.*, 2022). As noted by Chen *et al.* (2020), the macrocyclic and aromatic structures of chaetoglobosins are particularly well-suited for dual polar and hydrophobic binding, further reinforcing their potential as glycoprotein-directed antivirals.

Table 4: Post-Docking Interactions with RABV-G

Ligand	Protein-Ligand Docking Interaction	Binding Affinity (kcal/mol)	Interactions
11	 <p>Interactions</p> <ul style="list-style-type: none"> ■ Conventional Hydrogen Bond ■ Pi-Sigma ■ Carbon Hydrogen Bond ■ Pi-Alkyl 	-10.1	Hydrogen Bonding with Gln39, Gly42, and Gly100; π - π interactions with Val85 and Lys103; π -alkyl interactions with Val85 and Lys103.
9	 <p>Interactions</p> <ul style="list-style-type: none"> ■ Conventional Hydrogen Bond ■ Pi-Donor Hydrogen Bond ■ Carbon Hydrogen Bond ■ Pi-Sigma ■ Unfavorable Donor-Donor ■ Pi-Alkyl 	-9.9	Hydrogen Bonding with Asn26, Tyr315, and Ser23; π -donor hydrogen bonding with Lys313 and Asn26; π -sigma and π -alkyl interactions with Pro25, Lys306, Lys313, and Leu257
10	 <p>Interactions</p> <ul style="list-style-type: none"> ■ Conventional Hydrogen Bond ■ Pi-Sigma ■ Pi-Pi T-shaped ■ Alkyl ■ Pi-Alkyl 	-9.8	Hydrogen Bonding with Gly42, Gln42, and Gly100; Hydrophobic interactions with Val93, Phe95, and Lys103

Post-docking Analysis with RABV-L

Table 5: Post-Docking Interactions with RABV-L

Ligand	Protein-Ligand Docking Interaction	Binding Affinity (kcal/mol)	Interactions
11		-12.4	Hydrogen Bonding with Lys1182, Asn1185, and Glu1030; Electrostatic π -cation interaction with Arg1191; Hydrophobic π -alkyl contact with Arg1247
16		-11.1	Hydrogen Bonding with Lys980, Asn1185, Arg1191, and Glu1041; Carbon-hydrogen bonds with Ser915 and Ser1033; Hydrophobic π -alkyl interaction with Arg1247
12		-10.2	Hydrogen Bonding with Tyr1281 and Asp1282

The *Rabies lyssavirus* RNA-dependent RNA polymerase (RABV-L) plays a central role in viral transcription and replication, making it a main target for antiviral intervention (Albertini *et al.*, 2008). Molecular docking results revealed several fungal metabolites with notable binding affinities to RABV-L (Table 5), indicating their potential to disrupt polymerase function and thereby inhibit viral replication.

Chaetoglobosin C (**11**) exhibited the strongest binding affinity at -12.4 kcal/mol. Its interactions included hydrogen bonds with LYS1182, ASN1185, and GLU1030, complemented by a π -cation interaction with

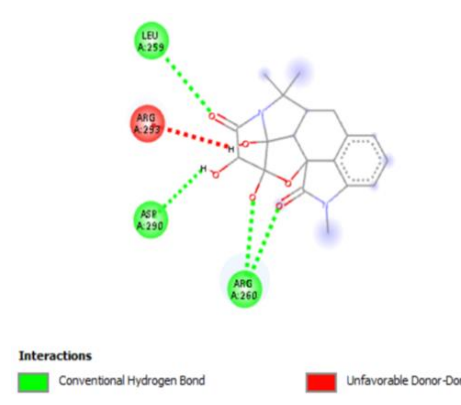
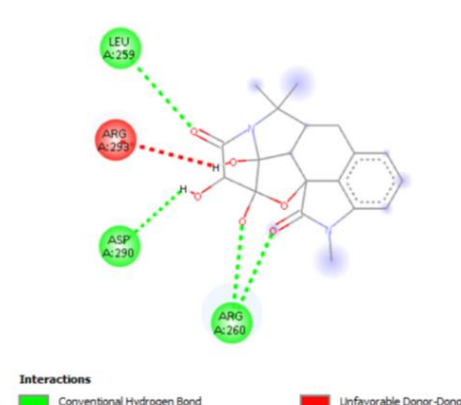
ARG1191 that contributed to electrostatic stability (Carter-Fenk *et al.*, 2023). Additional π -alkyl contacts with ARG1247 further reinforced ligand retention, indicating a highly stable binding configuration. Comparable binding modes, in which hydrogen bonding is combined with π -cation or hydrophobic interactions, have been reported for polymerase inhibitors targeting other RNA viruses, including the influenza virus PA and L polymerase complexes (Kouba *et al.*, 2019).

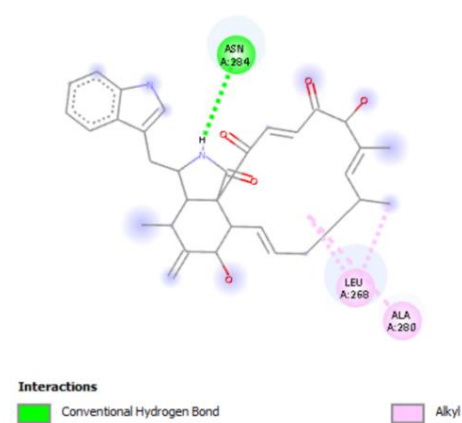
Chetomin (**16**), with a docking score of -11.1 kcal/mol, formed multiple hydrogen bonds (LYS980, ASN1185, ARG1191, GLU1041) together with carbon-hydrogen contacts (SER915, SER1033), collectively enhancing stability. π -Alkyl interactions with ARG1247 provided further reinforcement. Beyond its docking performance, Chetomin is recognised for its transcriptional regulatory effects, including inhibition of hypoxia-inducible factor-1 (HIF-1), and metabolites with related scaffolds have demonstrated inhibitory activity against flaviviral RNA polymerases (Obi *et al.*, 2021). Its predicted capacity to cross the blood-brain barrier (Bravo-Reyna *et al.*, 2024) further strengthens its therapeutic relevance for rabies, a neurotropic infection.

Chaetomugilin A (**12**), with a binding energy of -10.2 kcal/mol, formed hydrogen bonds with ASP1282 and TYR1281, interactions that contributed to stable docking within the active site. Similar hydrogen-bond-driven inhibition mechanisms have been documented for small molecules binding the RdRp active sites of Ebola virus (Li *et al.*, 2025), supporting Chaetomugilin A's potential as a polymerase-targeting antiviral.

Post-docking Analysis with RABV-P

Table 6: Post-Docking Interactions with RABV-P

Ligand	Protein-Ligand Docking Interaction	Binding Affinity (kcal/mol)	Interactions
1	 <p>Interactions</p> <ul style="list-style-type: none"> Conventional Hydrogen Bond Unfavorable Donor-Donor 	-7.9	Hydrogen bonds with residues LEU259, ARG260, and ASP290; Multiple hydrogen bonds from ARG260
11	 <p>Interactions</p> <ul style="list-style-type: none"> Conventional Hydrogen Bond Unfavorable Donor-Donor 	-7.9	Hydrogen bonds with LEU259:N (ligand O5), ARG260:NH2 (ligand O6 and O3), and ASP290:OD2 (ligand H15)

14	 <p>Interactions</p> <p> ■ Conventional Hydrogen Bond ■ Alkyl </p>	-7.9	<p>Conventional hydrogen bond between the donor :UNK1:H6 and the acceptor ASN284:OD1; Alkyl interactions between LEU268 and :UNK1, ALA280 and :UNK1, and LEU268 and :UNK1:C28</p>
----	--	------	---

The Rabies lyssavirus phosphoprotein (RABV-P) is essential for viral replication and immune evasion, acting both as a cofactor for the RNA-dependent RNA polymerase (RABV-L) and as an antagonist of interferon responses (Chelbi-Alix *et al.*, 2006). Molecular docking analysis identified Aspergilline A (**1**), Chaetoglobosin C (**11**), and Chaetoglobosin D (**14**) as potential inhibitors, each with a binding affinity of -7.9 kcal/mol (Table 6). The significance of targeting RABV-P lies in its dual functional domains; Sethi *et al.* (2023) demonstrated that the residues responsible for interferon antagonism overlap with those mediating polymerase binding, underscoring this protein as a particularly attractive antiviral target.

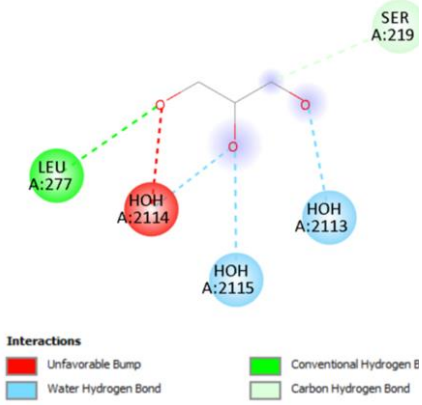
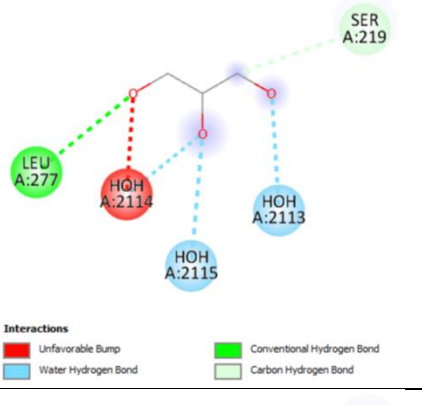
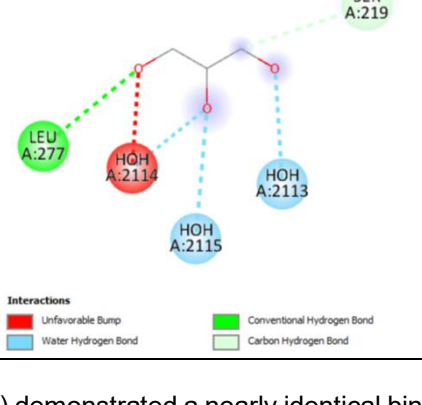
Aspergilline A (**1**) formed multiple hydrogen bonds with LEU259, ARG260, and ASP290, with ARG260 contributing several stabilising interactions. Notably, Rieder *et al.* (2011) reported that mutations in this region significantly impair RABV-P's capacity to inhibit interferon regulatory factor 3 (IRF-3), thereby diminishing viral immune evasion. This suggests that Aspergilline A may restore interferon signalling by disrupting phosphoprotein–host interactions, reinforcing its potential as an antiviral inhibitor.

Chaetoglobosin C (**11**) exhibited a comparable interaction profile, engaging ARG260, LEU259, and ASP290 through hydrogen bonding. In addition, alkyl interactions with LEU268 and ALA280 provided hydrophobic stabilization, which could disrupt conformational flexibility required for RABV-P function (Dar & Mir, 2017; Fu *et al.*, 2018). Chaetoglobosin derivatives have been previously reported by Alanzi *et al.* (2023) to establish stable hydrogen-bonding and hydrophobic contacts with viral surface proteins such as HIV gp120 and the SARS-CoV-2 spike glycoprotein, lending further support to their broad-spectrum antiviral potential.

Chaetoglobosin D (**14**) also bound within this pocket, forming a hydrogen bond with ASN284 and hydrophobic contacts with LEU268 and ALA280. While primarily recognized for its antifungal and antibacterial activities (Chen *et al.*, 2020), its ability to stabilize binding at these critical residues suggests a possible extension of its bioactivity into antiviral applications. Given the overlap in molecular pathways disrupted by Chaetoglobosin scaffolds, this compound may compromise RABV-P's role in replication and immune evasion.

Post-docking Analysis with RABV-M

Table 7: Post-Docking Interactions with RABV-M

Ligand	Protein-Ligand Docking Interaction	Binding Affinity (kcal/mol)	Interactions
10		-8.0	Hydrogen bonds mediated by GOL1297:O1 and GOL1297:O2 with water molecules (HOH2113, HOH2114, HOH2115); Conventional hydrogen bond with LEU277:O and a carbon-hydrogen bond with SER219:OG
17		-8.0	Hydrogen bonds between GOL1297:O1 and HOH2113:O, GOL1297:O2 and water molecules HOH2114 and HOH2115; Additional hydrogen bonds between GOL1297:O3 and LEU277:O, and GOL1297:C1 and SER219:OG.
11		-7.8	Hydrogen bonds mediated by GOL1297 with surrounding water molecules and residues LEU277 and SER219.

Stachybotrin C (**17**) demonstrated a nearly identical binding mode, with GOL1297 once again mediating hydrogen bonds at LEU277 and SER219. This repeated binding framework suggests that RABV-M harbours a conserved pocket particularly favourable for hydrogen bonding. Notably, conserved matrix protein binding regions have also been reported in the Ebola virus VP40, where repetitive hydrogen-bonding motifs form druggable hot spots that disrupt viral assembly (Bornholdt *et al.*, 2013).

Chaetoglobosin C (**11**) maintained the same hydrogen bond interactions, further reinforcing complex stability. As demonstrated by Barboro *et al.* (2012), structural disruptions in RABV-M's critical domains impair viral assembly, supporting the hypothesis that Chaetoglobosin derivatives could interfere with the protein's natural binding interfaces. Collectively, these findings suggest that Chaetoglobosin A, Stachybotrin C, and Chaetoglobosin C may inhibit rabies virus replication by obstructing key protein interactions essential for virion formation.

ADME and Physicochemical Profiles of the Targeted Fungal Metabolites

The ADME and physicochemical profiling of the targeted fungal metabolites was conducted using SwissADME and OSIRIS Property Explorer. Initially, eighteen (18) fungal metabolites were screened in silico to evaluate their absorption, distribution, metabolism, and excretion (ADME) properties. From this initial screening, the top-binding compounds (1, 9, 10, 11, 12, 14, 16, and 17) were further analyzed for drug-likeness, pharmacokinetic characteristics, and toxicity profiles.

Table 8: Physicochemical and Pharmacokinetic Properties of Fungal Metabolites using Lipinski's Rule of Five

Fungal Metabolites	Molecular Weight (<500 g/mol)	Num. H-bond Acceptors (<10)	Num. H-bond Donors (<5)	Lipophilicity MLOGP (<5)	Lipinski Num. Violations	Drug-likeness
Aspergilline A (1)	372.37	6	3	-0.15	0	Yes
Cladospirone B (9)	350.32	6	3	1.57	0	Yes
Chaetoglobosin A (10)	528.64	5	3	2.03	1	Yes
Chaetoglobosin C (11)	528.64	5	2	2.03	1	Yes
Chaetomugilin A (12)	450.91	7	2	1.38	0	Yes
Chaetoglobosin D (14)	528.64	5	4	1.96	1	Yes
Chetomin (16)	710.87	6	3	-0.19	2	No
Stachybotrin C (17)	505.65	5	3	3.60	1	Yes

Table 8 summarises the physicochemical profiles of the fungal metabolites based on Lipinski's Rule of Five, which provides a framework for predicting oral bioavailability. Aspergilline A (1) complied fully with the criteria, displaying a molecular weight of 372.37 g/mol, three hydrogen bond donors, six hydrogen bond acceptors, and an MLOGP of -0.15. This combination suggests excellent oral bioavailability, supported by its hydrophilic character, which enhances solubility in aqueous gastrointestinal environments, together with a moderate number of hydrogen bonding groups that promote interactions with biological targets without compromising permeability.

Cladospirone B (9) likewise exhibited no Lipinski violations, with a molecular weight of 350.32 g/mol, three hydrogen bond donors, six hydrogen bond acceptors, and an MLOGP of 1.57. Its slightly higher lipophilicity compared with Aspergilline A reflects a more balanced polarity, indicating good membrane permeability whilst retaining solubility, thereby supporting its suitability for oral administration.

Chaetoglobosin A (10) and Chaetoglobosin C (11) each demonstrated a single violation due to their relatively high molecular weights of 528.64 g/mol. Nonetheless, both compounds retained favourable lipophilicity and hydrogen bonding characteristics, which may allow for adequate bioavailability. Their elevated molecular weight may, however, limit intestinal absorption, suggesting that chemical modifications or formulation strategies could be employed to optimise oral delivery.

Chaetomugilin A (12), by contrast, adhered to all Lipinski criteria with a molecular weight of 450.91 g/mol, positioning it as a strong candidate for oral administration and further pharmacokinetic evaluation.

Although not explicitly discussed earlier, Chaetoglobosin D (14) is likely to follow a similar profile to Chaetoglobosins A and C, with a probable single violation based on molecular weight. Even so, its other physicochemical properties may compensate for this limitation, suggesting that oral activity could still be achievable under optimised conditions.

Chetomin (16) was the least favourable according to Lipinski's framework, exhibiting two violations resulting from its high molecular weight (710.87 g/mol) and excess hydrogen bond acceptors. Such properties are typically associated with reduced permeability and limited oral bioavailability. Its high

polarity further restricts passive intestinal absorption, indicating that alternative administration routes—such as intravenous delivery—may be required to realise its therapeutic potential.

Finally, Stachybotrin C (**17**) presented a single Lipinski violation while maintaining otherwise acceptable parameters. Although this may slightly reduce its permeability, the compound retains potential for further evaluation as a drug candidate.

BOILED-Egg Model

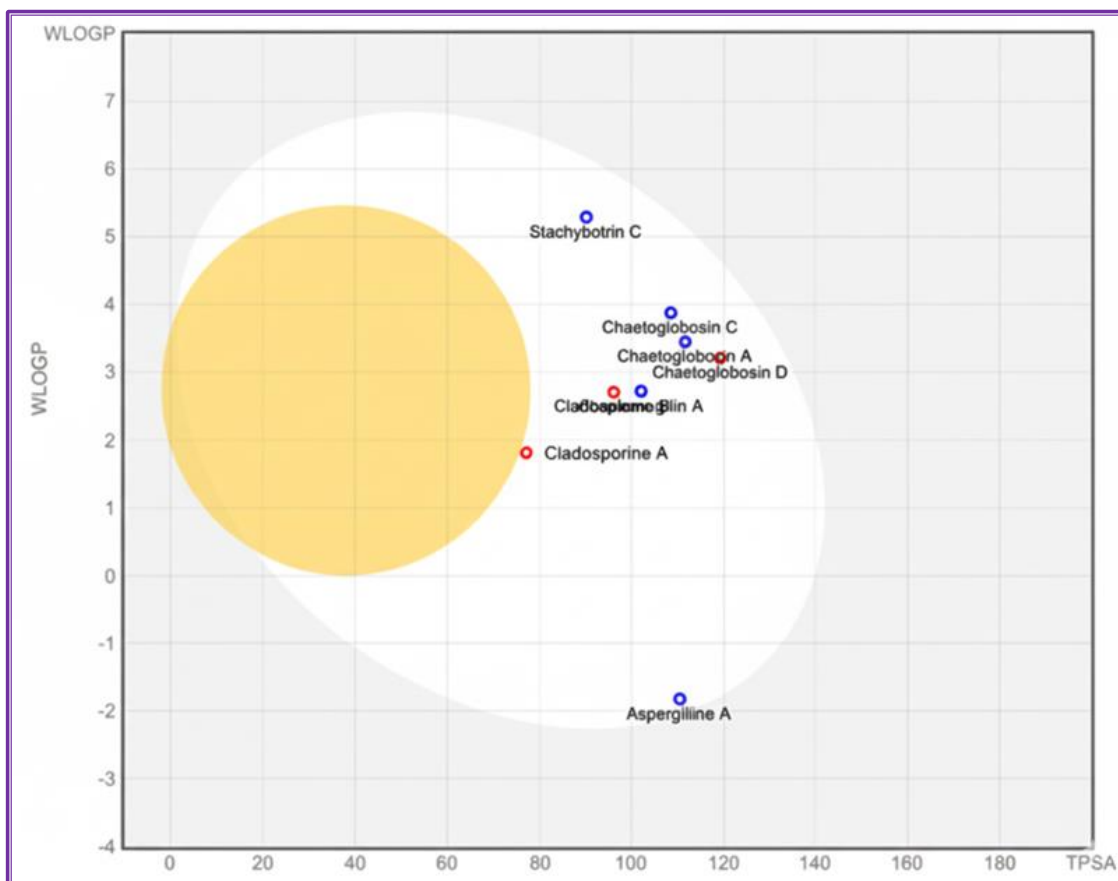


Figure 1: BOILED-egg Plot for the Prediction of GI Absorption and BBB Permeation of Compounds 1, 9, 10, 11, 12, 14, 16, and 17.

Figure 1 presents the BOILED-egg plot for gastrointestinal (GI) absorption and blood–brain barrier (BBB) permeation of compounds 1, 9, 10, 11, 12, 14, 16, and 17. All evaluated metabolites—Aspergilline A (1), Cladospirone B (9), Chaetoglobosin A (10), Chaetoglobosin C (11), Chaetomugilin A (12), Chaetoglobosin D (14), Chetomin (16), and Stachybotrin C (17)—were located within the egg-white region, indicating a high probability of passive GI absorption. This suggests that each of these compounds holds potential for oral administration.

In contrast, none of the compounds appeared in the yolk region, signifying limited ability to permeate the BBB. Such exclusion is generally attributed to elevated polarity or insufficient lipophilicity, factors that restrict passive diffusion across the highly selective BBB. Although this reduces the likelihood of direct central nervous system (CNS) activity, it does not preclude systemic therapeutic applications, particularly for viral infections where CNS penetration is not essential.

It is noteworthy that Chetomin (16), despite being positioned within the egg-white region, exhibited two violations of Lipinski's rules. These violations, arising from its high molecular weight and excess hydrogen-bond acceptors, may compromise its absorption and overall bioavailability. This suggests that structural modifications, aimed at reducing molecular size or hydrogen-bonding capacity, could be necessary to optimise Chetomin's oral drug-likeness.

*Toxicity and Pharmacological Properties of the Fungal Metabolites***Table 9: Toxicity Profiles of Compounds 1, 9, 10, 11, 12, 14, 16, and 17**

Fungal Metabolites	Mutagenicity	Tumorigenicity	Irritant Effect	Reproductive Toxicity
Aspergilline A (1)	none	none	none	none
Cladospirone B (9)	high risk	none	none	none
Chaetoglobosin A (10)	none	medium risk	medium risk	none
Chaetoglobosin C (11)	none	medium risk	medium risk	none
Chaetomugilin A (12)	none	none	high risk	none
Chaetoglobosin D (14)	none	none	none	none
Chetomin (16)	none	none	none	none
Stachybotrin C (17)	none	none	none	none

Table 9 summarises the predicted toxicity profiles of the top-binding fungal metabolites. Aspergilline A (**1**), Chaetoglobosin D (**14**), Chetomin (**16**), and Stachybotrin C (**17**) demonstrated no detectable toxicity risks across the evaluated parameters, including mutagenicity, tumourigenicity, irritancy, and reproductive toxicity. The absence of predicted toxicity in these compounds suggests that their molecular structures likely lack highly reactive functional groups, which are often responsible for DNA interaction or covalent modification of cellular macromolecules.

In contrast, Cladospirone B (**9**) was flagged for a high risk of mutagenicity. This finding raises concerns regarding its potential to induce genotoxic effects, either through direct DNA interaction or via the formation of reactive intermediates. A high mutagenicity risk significantly constrains its viability as a safe therapeutic scaffold unless targeted structural modifications are introduced to reduce or eliminate the genotoxic substructures, as suggested in previous studies on fungal metabolite optimisation (Chen *et al.*, 2020).

Chaetoglobosin A (**10**), Chaetoglobosin C (**11**), and Chaetomugilin A (**12**) were each predicted to carry moderate toxicity risks, particularly associated with irritant effects. Such outcomes may translate into local adverse reactions—for example, gastrointestinal irritation or dermal hypersensitivity—if administered without modification. While these findings do not preclude their potential as antiviral candidates, they highlight the necessity for structural refinement or formulation strategies to minimise irritancy whilst preserving binding affinity.

Discussion

This study systematically evaluated fungal metabolites against the four major rabies virus proteins L, G, M, and P, revealing patterns of binding, antiviral potency, pharmacokinetic behaviour, and predicted safety.

Among the four proteins, RABV-L consistently produced the strongest docking scores. Chaetoglobosin C, for example, bound at -12.4 kcal/mol, representing the lowest energy value among all compounds and targets, and also showed strong interaction with RABV-G (-10.1 kcal/mol). By contrast, its binding to RABV-P (-7.9 kcal/mol) and RABV-M (-7.8 kcal/mol) was comparatively moderate. The higher average affinity observed for RABV-L (-9.589 kcal/mol, Table 5) is likely attributable to the size and structural complexity of its polymerase active site. Larger binding cavities in polymerases can accommodate bulky metabolites such as Chaetoglobosins and Chetomin (molecular weight >500 g/mol, Table 4), enabling the formation of multiple hydrogen bonds and hydrophobic interactions simultaneously.

As Carter-Fenk *et al.* (2023) observed, molecular weight often correlates with enhanced complementarity to polymerase cavities, a trend reflected here in the moderate negative correlation between compound size and RABV-L docking score. Comparable patterns have been documented in

other RNA viruses: Kouba *et al.* (2019) demonstrated that large structures fit optimally within the influenza polymerase, while Li *et al.* (2025) reported similar findings for the Ebola virus polymerase. Moreover, the demonstrated susceptibility of flaviviral polymerases to small-molecule inhibitors confirms the druggability of viral RdRp domains (Obi *et al.*, 2021), thereby underscoring the translational relevance of the present findings.

In contrast, the RABV glycoprotein (RABV-G) demonstrated preferential binding towards smaller or moderately sized metabolites. Cladospirone B (molecular weight 350.32 g/mol) achieved a strong binding affinity of -9.9 kcal/mol, suggesting that the glycoprotein binding pocket is more size-selective and favours ligands with balanced polarity. Similar size-selective binding has been reported for SARS-CoV-2 spike protein inhibitors, where medium-sized fungal metabolites exhibited optimal affinity through a balance of polarity and lipophilicity (Alanzi *et al.*, 2023). Supporting this, Salvatore *et al.* (2021) highlighted the antiviral promise of *Cladosporium* metabolites, noting their structural compatibility with viral surface proteins. By contrast, the lower average scores obtained for RABV-M and RABV-P (Table 5) may reflect their shallower or less druggable binding sites, which limit the number of favourable interactions. Wang *et al.* (2023) similarly observed that accessory viral proteins often display lower druggability indices compared with catalytic polymerase domains. This observation is consistent with structural studies of Ebola VP40 (Bornholdt *et al.*, 2013) and the rabies phosphoprotein (Sethi *et al.*, 2023), both of which confirmed the challenges of targeting proteins with relatively featureless or dynamic binding surfaces.

When examining multi-target binding, Chaetoglobosin C again emerged as the most notable compound, displaying the lowest overall mean docking score (-9.55 kcal/mol, Table 5). However, its binding profile varied across the four proteins, with a high standard deviation of 1.885, reflecting strong complementarity with RABV-L but weaker interactions with M and P. This highlights both its strength as a polymerase inhibitor and its limitation as a broad-spectrum binder. Previous work by Chen *et al.* (2020) reinforces this selectivity, emphasising that chaetoglobosins preferentially target large catalytic domains rather than structural proteins, consistent with the present findings.

The ADMET analysis further contextualised these docking outcomes. Chaetoglobosins and Chetomin, despite their strong affinities, violated Lipinski's rules owing to their high molecular weight and lipophilicity, which likely enhance polymerase binding but compromise solubility and absorption. By contrast, Aspergilline A and Cladospirone B complied with Lipinski's criteria, explaining their predicted superior absorption (Table 6). As Leeson *et al.* (2021) observed, drug discovery often requires balancing binding potency with drug-likeness; here, stronger binding correlated with larger, less drug-like structures, whereas smaller, more drug-like molecules displayed reduced affinity. Notably, similar findings have been reported in SARS-CoV-2 studies by Qaisrani *et al.* (2021) and Alanzi *et al.* (2023), where bulky fungal alkaloids exhibited high affinity but poor pharmacokinetic potential compared with smaller metabolites.

Further limitations were revealed by the BOILED-egg predictions (Table 6). All metabolites demonstrated good gastrointestinal absorption but poor blood–brain barrier penetration, attributable to their large polar surface areas and lipophilicity. Roy *et al.* (2019) highlighted that while polar substituents promote oral solubility, they often impede CNS entry through passive diffusion. This is particularly relevant for rabies, given its neurotropic nature, as even Chaetoglobosin C—with excellent docking results—may fail to achieve effective CNS concentrations without modification or specialised delivery strategies. Such challenges are not unique: Doak *et al.* (2014) observed that large, polar antivirals targeting HIV and influenza polymerases often required nanoparticle carriers or prodrug strategies to achieve therapeutic CNS levels.

Toxicity predictions (Table 9) further underscored the necessity of balancing potency with safety. Cladospirone B, despite favourable binding and drug-likeness, was predicted to be mutagenic, likely due to reactive structural motifs. Chaetoglobosin A and C demonstrated moderate tumourigenicity and irritant properties, consistent with the reactivity of their macrocyclic skeletons and double bonds. By contrast, Aspergilline A, Chaetoglobosin D, and Chetomin showed no major toxicity alerts, highlighting

the variability in safety profiles across fungal metabolites. Importantly, Chen *et al.* (2020) previously cautioned that while chaetoglobosins possess potent antiviral activity, their structural reactivity may confer mutagenic risks, mirroring the present findings.

Conclusion

Rabies remains a universally fatal disease with no effective antiviral treatment, making the search for novel therapeutic options critical. In this study, fungal-derived metabolites were systematically evaluated as inhibitors of the four essential Rabies lyssavirus (RABV) proteins—glycoprotein (RABV-G), RNA-dependent RNA polymerase (RABV-L), phosphoprotein (RABV-P), and matrix protein (RABV-M). Molecular docking analysis revealed that several metabolites exhibited substantial binding affinities and stable *in silico* interactions with these targets, highlighting their potential as promising antiviral candidates.

Among the compounds tested, Chaetoglobosin C emerged as the most potent, achieving the strongest binding scores, particularly against RABV-L (−12.4 kcal/mol) and RABV-G (−10.1 kcal/mol), with an overall average affinity of −9.55 kcal/mol. Its ability to form multiple stabilising interactions suggests a strong inhibitory capacity. However, its relatively high molecular weight, violation of Lipinski's rules, and predicted medium-level toxicity raise concerns regarding its oral bioavailability and safety profile. These limitations may be addressed through rational chemical modifications—such as reducing lipophilicity or modifying reactive moieties—and through advanced formulation approaches to enhance central nervous system delivery.

Aspergilline A, by contrast, presents as a more drug-like candidate. It complies fully with Lipinski's criteria, demonstrates favourable predicted gastrointestinal absorption, and carries no significant toxicity alerts. While its binding affinity was lower than that of Chaetoglobosin C, its superior pharmacokinetic and safety profile make it a strong parallel candidate for further investigation. Cladospirone B also showed high affinity towards both RABV-G and RABV-L; however, its predicted mutagenicity significantly restricts its direct application. Future research should focus on structural modifications to eliminate genotoxic fragments while retaining binding capacity.

Taken together, these findings indicate that Chaetoglobosin C should be prioritised for validation against RABV-L and RABV-G, whilst Aspergilline A represents a safer lead structure with more favourable drug-like properties. Nevertheless, reliance on *in silico* predictions constitutes a limitation of the present work. *In vitro* and *in vivo* studies will be essential to confirm antiviral efficacy and to assess drug pharmacokinetics and toxicity.

Conflict of Interest

Authors declared no competing of interests.

Acknowledgement

The authors extend their acknowledgement to Far Eastern University for providing access to academic and computational resources that facilitated the successful completion of this study. Acknowledgement to RCSB Protein Data Bank, PubChem, UCSF Chimera, AutoDock Vina, SwissADME, and OSIRIS Property Explorer for offering open-access resources that were instrumental in conducting the study analyses.

References

- Alanzi, A. R., Parvez, M. K., & Al-Dosari, M. S. (2023). *In silico* identification of deep-sea fungal alkaloids as potential inhibitors of SARS-CoV-2, Delta and Omicron spikes. *Future Virology*, 18(14), 933-946. <https://doi.org/10.2217/fvl-2023-0102>
- Albertini, A. A. V., Schoehn, G., Weissenhorn, W., & Ruigrok, R. W. H. (2008). Structural aspects of rabies virus replication. *Cellular and Molecular Life Sciences*, 65(2), 282-294. <https://doi.org/10.1007/s00018-007-7298-1>
- Barboro, P., Repaci, E., D'Arrigo, C., & Balbi, C. (2012). The role of nuclear matrix proteins binding to matrix

- attachment regions (Mars) in prostate cancer cell differentiation. *PloS One*, 7(7), e40617. <https://doi.org/10.1371/journal.pone.0040617>
- Bornholdt, Z. A., Noda, T., Abelson, D. M., Halfmann, P., Wood, M. R., Kawaoka, Y., & Saphire, E. O. (2013). Structural rearrangement of ebola virus VP40 begets multiple functions in the virus life cycle. *Cell*, 154(4), 763-774. <https://doi.org/10.1016/j.cell.2013.07.015>
- Bravo-Reyna, C. C., Miranda-Galván, V., Reyes-Soto, G., Vicuña, R., Alanis-Mendizabal, J., Escobar-Valderrama, M., ... & Torres-Villalobos, G. (2024). Evaluation of the Chetomin effect on histopathological features in a murine acute spinal cord injury model. *World Neurosurgery: X*, 25, 100414. <https://doi.org/10.1016/j.wnsx.2024.100414>
- Carter-Fenk, K., Liu, M., Pujal, L., Loipersberger, M., Tsanai, M., Vernon, R. M., ... & Head-Gordon, T. (2023). The energetic origins of pi-pi contacts in proteins. *Journal of the American Chemical Society*, 145(45), 24836-24851. <https://doi.org/10.1021/jacs.3c09198>
- Chelbi-Alix, M. K., Vidy, A., Bougrini, J. E., & Blondel, D. (2006). Rabies viral mechanisms to escape the IFN system: the viral protein P interferes with IRF-3, Stat1, and PML nuclear bodies. *Journal of Interferon & Cytokine Research*, 26(5), 271-280. <https://doi.org/10.1089/jir.2006.26.271>
- Chen, J., Zhang, W., Guo, Q., Yu, W., Zhang, Y., & He, B. (2020). Bioactivities and future perspectives of Chaetoglobosins. *Evidence-Based Complementary and Alternative Medicine*, 2020(1), 8574084. <https://doi.org/10.1155/2020/8574084>
- Dar, A. M., & Mir, S. (2017). Molecular docking: approaches, types, applications and basic challenges. *Journal of Analytical & Bioanalytical Techniques*, 8(2), 1-3. <https://doi.org/10.4172/2155-9872.1000356>
- Desantis, F., Miotto, M., Di Rienzo, L., Milanetti, E., & Ruocco, G. (2022). Spatial organization of hydrophobic and charged residues affects protein thermal stability and binding affinity. *Scientific Reports*, 12(1), 12087. <https://doi.org/10.1038/s41598-022-16338-5>
- Doak, B. C., Over, B., Giordanetto, F., & Kihlberg, J. (2014). Oral druggable space beyond the rule of 5: insights from drugs and clinical candidates. *Chemistry & Biology*, 21(9), 1115-1142. <https://doi.org/10.1016/j.chembiol.2014.08.013>
- Fatima, M., Iqbal, T., Shaheen, L., Salma, U., Siddique, R., Ali, R., ... & Usman, S. (2023). Transmission dynamics of rabies virus. *International Journal of Agriculture and Biosciences*, 3, 386-397. <https://doi.org/10.47278/book.zoon/2023.110>
- Fisher, C. R., Streicker, D. G., & Schnell, M. J. (2018). The spread and evolution of rabies virus: conquering new frontiers. *Nature Reviews Microbiology*, 16(4), 241-255. <https://doi.org/10.1038/nrmicro.2018.11>
- Fu, Y., Zhao, J., & Chen, Z. (2018). Insights into the molecular mechanisms of protein-ligand interactions by molecular docking and molecular dynamics simulation: a case of oligopeptide binding protein. *Computational and Mathematical Methods in Medicine*, 2018(1), 3502514. <https://doi.org/10.1155/2018/3502514>
- Kimitsuki, K., Khan, S., Kaimori, R., Yahiro, T., Saito, N., Yamada, K., ... & Nishizono, A. (2023). Implications of the antiviral drug favipiravir on rabies immunoglobulin for post-exposure prophylaxis of rabies in mice model with category III-like exposures. *Antiviral Research*, 209, 105489. <https://doi.org/10.1016/j.antiviral.2022.105489>
- Kouba, T., Drncova, P., & Cusack, S. (2019). Structural snapshots of actively transcribing influenza polymerase. *Nature Structural & Molecular Biology*, 26(6), 460-470. <https://doi.org/10.1038/s41594-019-0232-z>
- Lee, M. F., Wu, Y. S., & Poh, C. L. (2023). Molecular mechanisms of antiviral agents against dengue virus. *Viruses*, 15(3), 705. <https://doi.org/10.3390/v15030705>
- Leeson, P. D., Bento, A. P., Gaulton, A., Hersey, A., Manners, E. J., Radoux, C. J., & Leach, A. R. (2021). Target-based evaluation of "drug-like" properties and ligand efficiencies. *Journal of medicinal chemistry*, 64(11), 7210-7230. <https://doi.org/10.1021/acs.jmedchem.1c00416>
- Li, G., Du, T., Wang, J., Jie, K., Ren, Z., Zhang, X., ... & Ru, H. (2025). Structural insights into the RNA-dependent RNA polymerase complexes from highly pathogenic Marburg and Ebola viruses. *Nature Communications*, 16(1), 3080. <https://doi.org/10.1038/s41467-025-58308-1>
- Lian, M., Hueffer, K., & Weltzin, M. M. (2022). Interactions between the rabies virus and nicotinic acetylcholine receptors: A potential role in rabies virus induced behavior modifications. *Heliyon*, 8(9), e10434. <https://doi.org/10.1016/j.heliyon.2022.e10434>
- Ling, M. Y. J., Halim, A. F. N. A., Ahmad, D., Ramly, N., Hassan, M. R., Rahim, S. S. S. A., ... & Hidrus, A. (2023). Rabies in Southeast Asia: a systematic review of its incidence, risk factors and mortality. *BMJ Open*, 13(5), e066587. <https://doi.org/10.1136/bmjopen-2022-066587>
- Lipinski, C. A., Lombardo, F., Dominy, B. W., & Feeney, P. J. (2001). Experimental and computational approaches to estimate solubility and permeability in drug discovery and development settings. *Advanced drug delivery reviews*, 46(1-3), 3-26. [https://doi.org/10.1016/s0169-409x\(00\)00129-0](https://doi.org/10.1016/s0169-409x(00)00129-0)

- Louten, J. (2016). Virus replication. In *Essential Human Virology* (pp. 49–70). Elsevier. <https://doi.org/10.1016/b978-0-12-800947-5.00004-1>
- Obi, J., Gutiérrez-Barbosa, H., Chua, J., & Deredge, D. (2021). Current trends and limitations in dengue antiviral research. *Tropical Medicine and Infectious Disease*, 6(4), 180. <https://doi.org/10.3390/tropicalmed6040180>
- Petterson, E. F., Goddard, T. D., Huang, C. C., Couch, G. S., Greenblatt, D. M., Meng, E. C., & Ferrin, T. E. (2004). UCSF Chimera—a visualization system for exploratory research and analysis. *Journal of Computational Chemistry*, 25(13), 1605-1612. <https://doi.org/10.1002/jcc.20084>
- Qaisrani, M. N., Belousov, R., Rehman, J. U., Goliaei, E. M., Giroto, I., Franklin-Mergarejo, R., ... & Roldan, E. (2021). Phospholipids dock SARS-CoV-2 spike protein via hydrophobic interactions: A minimal in-silico study of lecithin nasal spray therapy. *The European Physical Journal E*, 44(11), 132. <https://doi.org/10.1140/epje/s10189-021-00137-3>
- Quiambao, B., Varghese, L., Demarteau, N., Sengson, R. F., Javier, J., Mukherjee, P., ... & Preiss, S. (2020). Health economic assessment of a rabies pre-exposure prophylaxis program compared with post-exposure prophylaxis alone in high-risk age groups in the Philippines. *International Journal of Infectious Diseases*, 97, 38-46. <https://doi.org/10.1016/j.ijid.2020.05.062>
- Rampersad, S., & Tennant, P. (2018). Replication and Expression Strategies of Viruses. *Viruses*, 55–82. <https://doi.org/10.1016/b978-0-12-811257-1.00003-6>
- Rieder, M., Brzózka, K., Pfaller, C. K., Cox, J. H., Stitz, L., & Conzelmann, K. K. (2011). Genetic dissection of interferon-antagonistic functions of rabies virus phosphoprotein: inhibition of interferon regulatory factor 3 activation is important for pathogenicity. *Journal of virology*, 85(2), 842-852. <https://doi.org/10.1128/jvi.01427-10>
- Roy, D., Hinge, V. K., & Kovalenko, A. (2019). To pass or not to pass: predicting the blood–brain barrier permeability with the 3D-RISM-KH molecular solvation theory. *ACS Omega*, 4(16), 16774-16780. <https://doi.org/10.1021/acsomega.9b01512>
- Salvatore, M. M., Andolfi, A., & Nicoletti, R. (2021). The genus *Cladosporium*: A rich source of diverse and bioactive natural compounds. *Molecules*, 26(13), 3959. <https://doi.org/10.3390/molecules26133959>
- Sethi, A., Rawlinson, S. M., Dubey, A., Ang, C. S., Choi, Y. H., Yan, F., ... & Gooley, P. R. (2023). Structural insights into the multifunctionality of rabies virus P3 protein. *Proceedings of the National Academy of Sciences*, 120(14), e2217066120. <https://doi.org/10.1073/pnas.2217066120>
- Song, X. (2024). Antibacterial, antifungal, and antiviral bioactive compounds from natural products. *Molecules*, 29(4), 825. <https://doi.org/10.3390/molecules29040825>
- Wang, Z. Z., Shi, X. X., Huang, G. Y., Hao, G. F., & Yang, G. F. (2023). Fragment-based drug discovery supports drugging ‘undruggable’ protein–protein interactions. *Trends in Biochemical Sciences*, 48(6), 539-552. <https://doi.org/10.1016/j.tibs.2023.01.008>
- World Health Organization (2024). *Rabies* (Fact sheet). <https://www.who.int/news-room/fact-sheets/detail/rabies>
- Yuan, Y., Fang, A., Wang, H., Wang, C., Sui, B., Zhao, J., ... & Zhao, L. (2024). Lyssavirus M protein degrades neuronal microtubules by reprogramming mitochondrial metabolism. *Mbio*, 15(3), e02880-23. <https://doi.org/10.1128/mbio.02880-23>
- Zhan, J., Chakraborty, S., Sethi, A., Mok, Y. F., Yan, F., Moseley, G. W., & Gooley, P. R. (2025). Analysis of mechanisms of the rabies virus P protein-nucleocapsid interaction using engineered N-protein peptides and potential applications in antivirals design. *Antiviral Research*, 234, 106075. <https://doi.org/10.1016/j.antiviral.2024.106075>
- Zhang, S., Krumberger, M., Morris, M. A., Parrocha, C. M. T., Kreutzer, A. G., & Nowick, J. S. (2021). Structure-based drug design of an inhibitor of the SARS-CoV-2 (COVID-19) main protease using free software: A tutorial for students and scientists. *European Journal of Medicinal Chemistry*, 218, 113390. <https://doi.org/10.1016/j.ejmech.2021.113390>